Power System Operational Adequacy Evaluation with Wind Power Ramp Limits

Yuzhong Gong, *Member IEEE*, C. Y. Chung, *Fellow*, *IEEE,* and R. S. Mall

***Abstract*—Uncertainties associated with wind power integration challenge the operational adequacy of conventional power systems. A set of wind power ramp limits (WPRLs) is proposed in this paper to evaluate the operational adequacy of power systems with high wind power penetration and to provide operating references to wind farms in the form of a ramp power limit (RPL) and ramp rate limit (RRL). The RPL is used to evaluate the minimum and maximum allowable generation of a wind farm by considering the power reserve capacities of generators and power flow constraints of transmission lines. A robust second-order cone programming (SOCP) RPLs formulation with AC power flow constraints and a column-and-constraint generation (C&CG) based solution method are proposed to maximize the total operating range of all wind farms. Meanwhile, a Pareto optimality-based RPLs evaluation approach is proposed to handle the coupled relationship among the operating ranges of the wind farms to achieve a balanced RPLs solution for each wind farm. The RRL is used to evaluate the most rapid wind power ramp behavior that can be handled by system frequency regulation without exceeding the designated frequency range. A comprehensive criterion is proposed to evaluate the RRLs by considering primary and secondary frequency regulation. Finally, the effectiveness of the proposed evaluation approach is verified through case studies.**

***Index Terms*—Adequacy evaluation; Pareto optimality; wind power ramp limits (WPRLs); ramp power limit (RPL); ramp rate limit (RRL).**

NOMENCLATURE

Sets and Indices:

W	Set of wind farms.
G	Set of generation units.
B	Set of buses.
L	Set of transmission lines.
$\delta(n)$	Set of neighbor buses of bus n.
$i(n)$	Index for wind farm i located at bus n.
$j(n)$	Index for generator j located at bus n.

Parameters:

$P_{\mathrm{W},i}^{t_0}$	Current power output of wind farm i.
$C_{\mathrm{W},i}$	Rated capacity of wind farm i.
C_{W}	Total capacity of integrated wind farms.
T_1	Time interval for evaluation of RRL.
T_2	Time interval for evaluation of RPL.
Δt_{d}	Time delay of AGC.
$P_{\mathrm{G},i}^{t_0}$	Current power output of generator j.
$P_{\mathrm{G},j}^{\max}$, $P_{\mathrm{G},j}^{\min}$	Active power output bound of generator j.
$Q_{\mathrm{G},j}^{\max}$, $Q_{\mathrm{G},j}^{\min}$	Reactive power output bound of generator j.
$dP_{\mathrm{G},j}$	Active power ramp rate of generator j.
$P_{\mathrm{G},j}^{\mathrm{up}}$, $P_{\mathrm{G},j}^{\mathrm{dn}}$	Bound of active power from generator j in upcoming period T_2.
$C_{\mathrm{reg},j}^{\mathrm{up}}$, $C_{\mathrm{reg},j}^{\mathrm{dn}}$	Upward and downward active power capacity of generator j participating in primary frequency regulation.
$V_n^{\max}$, $V_n^{\min}$	Voltage bound of bus n.
$P_{\mathrm{D},n}^t$, $Q_{\mathrm{D},n}^t$	Active and reactive load demand at bus n.
$G_{nm} + jB_{nm}$	The transfer admittance between bus n and m.
FL_{nm}	Capacity of transmission line between bus n and bus m.
R_j	Frequency regulation droop of generator j.
M	Inertia constant of power system.
D	Load damping coefficient.
Δf_{ub}, Δf_{lb}	Bound of frequency deviation.

Variables:

$L_{\mathrm{RP},i}^{+}$	Positive ramp power limit for wind farm i.
$L_{\mathrm{RP},i}^{-}$	Negative ramp power limit for wind farm i.
L_{RR}^{+}	Positive ramp rate limit for wind farms.
L_{RR}^{-}	Negative ramp rate limit for wind farms.
$P_{\mathrm{W},i}^t$	Active power output of wind farm i.
$P_{\mathrm{G},j}^t$	Active power output of generator j.
c_{nm}, s_{nm}	Ancillary variables for power flow formulation.
ΔP_{W}^t	Change of total wind power generation.
ΔP_{D}^t	Change of total active power load demand.
$\Delta P_{\mathrm{ref},j}^t$	Change of active power reference of generator j.
$\Delta P_{\mathrm{reg},j}^t$	Primary regulation response of generator j.

This work was supported in part by the Natural Sciences and Engineering Research Council of Canada (NSERC) and the Saskatchewan Power Corporation (SaskPower).

Yuzhong Gong and C.Y Chung are with the Department of Electrical and Computer Engineering, University of Saskatchewan, Saskatoon, SK S7N 5A9, Canada (e-mail: y.z.gong@usask.ca; c.y.chung@usask.ca).

R. S. Mall is with the Saskatchewan Power Corporation (SaskPower), Regina, SK S4P 0S1, Canada (e-mail: rmal@saskpower.com).

I. INTRODUCTION

POWER system operations primarily focus on supplying sufficient electrical energy to customers at a high level of security, high level of reliability, and at the lowest possible cost. Acceptable operation of a power system requires that generation and demand always be balanced in order to keep the system frequency nearly constant. The increasing penetration of wind power introduces more uncertainties to power systems, which challenges their real-time operation [1]. Several

approaches have been implemented to improve power system operational adequacy with wind power integration, such as stochastic or robust unit commitment (UC) [2], [3], risk management-based economic dispatch (ED) [4], robust optimal power flow (OPF) [5], [6], and application of energy storage systems (ESSs) [7].

Due to limited spinning reserves and frequency regulation resources, the capability of a power system to handle wind power uncertainties is limited. Thus, different grid codes have been presented by power system operators to regulate wind power integration [8], in which the active power output of the wind farm is one of the most important aspects. In Nordic, wind farms are required to control the change of power output caused by increased wind speed to less than 10% of the rated power capacity per minute [9]. In EirGrid, active power control set-points and their ramp rates are also advised by the transmission system operator (TSO) [10]. Constant wind power ramp criteria can reduce the impact of wind power uncertainty on power system operational security and reliability but cannot indicate the actual limit of power system operational adequacy for handling wind power uncertainty.

Considering the limited capability of the power system and the unavoidable wind power prediction error, an accurate evaluation of wind power ramp limits (WPRLs) based on real-time power system conditions can provide operating references for wind farms and also help system operators to realize better power system scheduling. The Independent System Operator New England (ISO-NE) introduced the concept of Do-Not-Exceed (DNE) limits for variable resources to facilitate real-time dispatch [11]. The maximum total operating range of all wind farms that the power system can accommodate without sacrificing system reliability is identified with a robust linear optimization formulation. The worst case of wind power outputs from different wind farms under the DNE limits is considered through the robust optimization method, neglecting the correlation among power outputs from different wind farms. In [12], a day-ahead robust linear topology control (RTC) formulation is proposed to enhance the DNE limits by managing the power flow congestion, which can result in a 22%~26% increase in DNE limits. However, the DNE limits formulations presented in both [11] and [12] are based on the DC power flow without considering power losses and reactive power transfer. An AC power flow formulation [13] can improve the accuracy of the allowed operating ranges evaluation for wind farms, but would lead to a robust conic optimization problem.

To solve a robust linear optimization problem, the Benders' decomposition algorithm is widely applied to divide the original optimization problem into a master problem and a subproblem and solve it with a number of iterations [14]-[16]. In [11], the affine policy with optimal and fixed participation factors of generators is applied to solve the DNE limits problem with lower implementation difficulty. A multistage solution method is developed in [12] to solve the RTC DNE limits problem through an iterative procedure based on the duality theory and the big-M method. The column-and-constraint generation (C&CG) method proposed in [17] performs better than the Benders' decomposition algorithm with respect to computational time and number of iterations when solving a robust linear optimization; this approach can also be implemented efficiently in robust conic optimization.

Moreover, only the maximum total operating range of all wind farms is considered as the objective function in the DNE limits formulation. Failing to consider the different current power outputs, rated capacities, and locations of wind farms will result in quite different operating ranges for different wind farms [11]. When the dispatchable resources for handling wind power uncertainty shared by all wind farms are limited, some wind farms would receive relatively narrower operating ranges compared to others, even including no ramping up or ramping down permissions. The unbalanced operating ranges obtained can neither reflect the accurate operational adequacy of power systems nor provide the actual operating restrictions to wind farm operators. To obtain a balanced evaluation result, the coupled relationship among the allowed operating ranges of different wind farms due to sharing the power reserve capacity and available transfer capacities (ATCs) of transmission lines should be properly handled while maximizing the total operating range. Therefore, the ramp power limit (RPL) is introduced in this paper to represent the operating range of a wind farm based on the current power output and rated power capacity of that wind farm.

In addition to operating ranges, the wind power ramp rate is another important criterion that needs to be considered in power systems with high wind power penetration [18]. If wind power fluctuates with a very high ramp rate, the system frequency would temporarily exceed the designated range even if the amplitude is still within the operating range. The impact of wind power ramp events on grid frequency deviation is investigated in [19] and the wind power penetration limited by the frequency deviation is evaluated in [20]. According to the frequency response characteristic of a power system, the frequency deviation caused by a wind power ramp event depends not only on the wind power penetration and ramp rate but also the system inertia [21], primary frequency regulation (PFR) [22], and automatic generation control (AGC) [19].

However, minimal literature discusses the real-time evaluation of the wind power ramp rate limit (RRL). Most of the research on wind power ramp control uses the constant RRLs from the grid codes [18]. In [23], the RRL is adjusted by a penalty function after analyzing the relationship between the wind power ramp rate and the required amount of ancillary service. This strategy can reduce the implementation difficulty of wind power ramp rate control, compared to the simple constant RRL, but still cannot keep the grid frequency deviation within a designated range as the RRL is not evaluated based on real-time operating conditions. The frequency response of a generator tripping event is analyzed in [24] to obtain a criterion of the minimum ramping capability of the overall system governors to ensure the frequency nadir within the designed range. For a sudden loss of generation, the frequency nadir would occur a short time after the event, which is mainly affected by the inertia of the power system and the ramping capability of the PFR. However, the frequency response of wind power ramping is different, as the duration of power change can be as long as minutes or even hours and the maximum frequency deviation not only depends on the total power loss but also the ramp rate. Due to the long duration, the implementation of PFR and AGC should be considered together to evaluate the wind power ramp limit.

As discussed above, both the amplitude and ramp rate of the wind power should be considered to evaluate the operational adequacy of the power system and provide operating references for wind farms. To address this issue, a set of WPRLs is proposed and evaluated in this paper, including the RPL and the RRL. The RPL represents the restriction on power change from wind power generation, which is mainly related to the spinning reserve capacity and the power flow constraints. The RRL is evaluated by considering the frequency regulation capability of the power system, which means the most rapid wind power ramp behavior that can be accommodated while keeping the system frequency deviation within the designated range.

The contributions of this paper include the following:

1) A robust second-order cone programming (SOCP) RPLs formulation is proposed to evaluate the maximum operating ranges for wind farms with AC power flow constraints. A C&CG-based solution method is applied to effectively solve the RPL problem.
2) A Pareto optimality-based approach is proposed to realize a balanced RPLs solution for each wind farm by considering the individual operating ranges of different wind farms while maximizing the total operating range.
3) A comprehensive criterion for RRLs is introduced to evaluate the unified RRLs for all wind farms to restrict the grid frequency deviation, based on the obtained RPLs and the capability of power system frequency regulation.

The remainder of the paper is organized as follows. Section II describes the concept and evaluation process of WPRLs. The mathematical model and solution methods of the RPLs problem are proposed in Section III. The analysis of frequency response to wind power ramp events and criteria to evaluate RRLs are discussed in Section IV. In Section V, two case studies employing a modified IEEE 9-bus system and a modified UIUC 150-bus system are presented to verify the proposed approach. Section VI provides the conclusions.

II. Definition and Evaluation of WPRLs

A. Definition of WPRLs

Power system operations aim to maintain the ability of the system to provide enough reserve capacity and have a sufficient response rate for potential power imbalances. This can be described as the power system ramp capacity, and includes ramp power capacity and ramp rate capacity [25]. In power systems with high wind power penetration, the power balance is disturbed when wind power ramp behavior beyond the power system ramp capability occurs. Based on the ramp capability, two out-of-limit situations for wind power ramp behavior, i.e., ramp power out-of-limit and ramp rate out-of-limit, might also occur as shown in Fig. 1. The former results from the insufficiency of power reserves to regulate generators to compensate for the change in wind power or from the power outputs of generators being restricted by the ATCs of the transmission lines. The latter is because the change of wind power is too rapid and the frequency regulation capability is not sufficient to maintain the system frequency within the designated range.

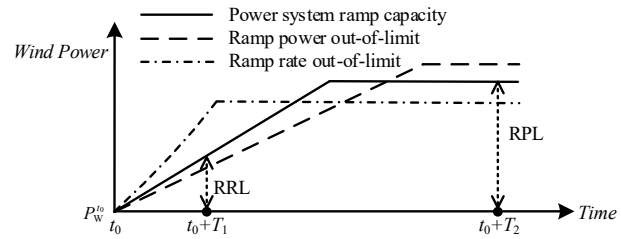

Fig. 1. Power system ramp capacity and out-of-limit situations.

To consider both the magnitude and ramp rate of a wind power ramp event, the mathematical definition of wind power ramp limits is presented as follows:

$$\begin{cases} L_{\mathrm{RP}}^{-} \le \dfrac{P_{\mathrm{W}}^{t} - P_{\mathrm{W}}^{t_0}}{C_{\mathrm{W}}} \le L_{\mathrm{RP}}^{+}, \forall t \in \left[t_0, t_0 + T_2\right] \\ L_{\mathrm{RR}}^{-} \le \dfrac{P_{\mathrm{W}}^{t+T_1} - P_{\mathrm{W}}^{t}}{C_{\mathrm{W}} T_1} \le L_{\mathrm{RR}}^{+}, \forall t \in \left[t_0, t_0 + T_2\right] \end{cases} \tag{1}$$

where L_{RP}^{+} and L_{RP}^{-}represent the positive and negative RPLs, respectively, and L_{RR}^{+} and L_{RR}^{-} represent the positive and negative RRLs, respectively.

In this paper, T_1= 5 minutes and T_2 = 30 minutes. To avoid conflicts, the RPLs and RRLs should satisfy the following relationship:

$$\begin{cases} L_{\mathrm{RR}}^{+} \ge L_{\mathrm{RP}}^{+} / T_2 \ge 0 \\ L_{\mathrm{RR}}^{-} \le L_{\mathrm{RP}}^{-} / T_2 \le 0 \end{cases} \tag{2}$$

B. Evaluation of WPRLs

In power system operation scheduling, several approaches at different time scales are performed to dispatch resources and maintain the balance between power generation and demand, as shown in Fig. 2.

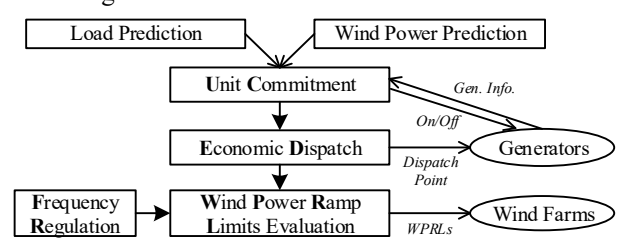

Fig. 2. Flowchart of wind power ramp limits evaluation.

The on/off states and dispatch points (power references) of generators are decided by UC and ED, respectively, based on load prediction and wind power prediction, while frequency regulation adjusts the power outputs of generators based on the real-time frequency deviation. With the determined on/off states, dispatch points, and frequency regulation characteristics of the generators, evaluation of the WPRLs can provide an estimate of power system ramp capacity and operating references for wind farms. It is crucial to maintain reasonable WPRLs for wind farms to fully utilize the wind power generation and ensure operational security and flexibility. Stringent WPRLs caused by prediction errors or contingencies can also indicate that the generators need to be re-dispatched to ensure the operational adequacy of the power system.

III. Evaluation of RPLs

Evaluating the RPLs of different wind farms can be conceptually considered as finding the largest uncertainty in

wind power that can be handled by a power system without sacrificing system security and reliability. In this section, a robust conic formulation of the RPLs problem and a C&CG-based solution method are proposed to obtain the allowed maximum RPLs solution for wind farms. Due to the fact that different wind farms share system spinning reserve and ATCs of transmission lines, there is a coupled relationship among the RPLs of different wind farms. Therefore, a RPLs evaluation approach based on Pareto optimality is proposed to take account of the individual operating range of each wind farm.

A. RPLs Model

The RPLs problem needs to find the minimum negative RPLs and maximum positive RPLs for wind farms, while satisfying the constraints from the generators and transmission network with all possible wind power outputs under those RPLs. As the power flow solution should be decided after the uncertainty realization of wind power outputs, the RPLs problem is a robust optimization with resource problem. Therefore, a three-stage robust optimization formulation is presented as follows:

$$\min_{L^{+}_{\mathrm{RP},i},L^{-}_{\mathrm{RP},i}}\left[\sum_{i\in\mathbf{W}}\left(L^{-}_{\mathrm{RP},i}-L^{+}_{\mathrm{RP},i}\right)+\max_{P^{t}_{\mathrm{W},i}\in\mathbf{O}}\ \min_{\substack{P^{t}_{\mathrm{G},j},Q^{t}_{\mathrm{G},j},p_{nm},\\ q_{nm},c_{nm},s_{nm}}} 0\right] \tag{3}$$

$$s.t.\quad 0\le L^{+}_{\mathrm{RP},i}\le 1-P^{t_0}_{\mathrm{W},i}/C_{\mathrm{W},i},\ i\in\mathbf{W} \tag{4}$$

$$-P^{t_0}_{\mathrm{W},i}/C_{\mathrm{W},i}\le L^{-}_{\mathrm{RP},i}\le 0,\ i\in\mathbf{W} \tag{5}$$

$$P^{\mathrm{dn}}_{\mathrm{G},j}\le P^{t}_{\mathrm{G},j}\le P^{\mathrm{up}}_{\mathrm{G},j},\ j\in\mathbf{G} \tag{6}$$

$$Q^{\min}_{\mathrm{G},j}\le Q^{t}_{\mathrm{G},j}\le Q^{\max}_{\mathrm{G},j},\ j\in\mathbf{G} \tag{7}$$

$$\left(V^{\min}_{n}\right)^2\le c_{nn}\le\left(V^{\max}_{n}\right)^2,\ n\in\mathbf{B} \tag{8}$$

$$P^{t}_{\mathrm{W},i(n)}+P^{t}_{\mathrm{G},j(n)}-P^{t}_{\mathrm{D},n}=g_{nn}c_{nn}+\sum_{m\in\delta(n)}p_{nm},\ n\in\mathbf{B} \tag{9}$$

$$Q^{t}_{\mathrm{G},j(n)}-Q^{t}_{\mathrm{D},n}=-b_{nn}c_{nn}+\sum_{m\in\delta(n)}q_{nm},\ n\in\mathbf{B} \tag{10}$$

$$p_{nm}=-G_{nm}c_{nn}+G_{nm}c_{nm}-B_{nm}s_{nm},\ (n,m)\in\mathbf{L} \tag{11}$$

$$q_{nm}=B_{nm}c_{nn}-B_{nm}c_{nm}-G_{nm}s_{nm},\ (n,m)\in\mathbf{L} \tag{12}$$

$$c_{nm}-c_{mn}=0,\ (n,m)\in\mathbf{L} \tag{13}$$

$$s_{nm}+s_{mn}=0,\ (n,m)\in\mathbf{L} \tag{14}$$

$$c^2_{nm}+s^2_{nm}\le c_{nn}c_{mm},\ (n,m)\in\mathbf{L} \tag{15}$$

$$p^2_{nm}+q^2_{nm}\le FL_{nm},\ (n,m)\in\mathbf{L} \tag{16}$$

where

$$\mathbf{O}=\left\{P_{\mathrm{W},i}\in\mathbf{R}^{\mathbf{W}}:P^{t_0}_{\mathrm{W},i}+L^{-}_{\mathrm{RP},i}C_{\mathrm{W},i}\le P^{t}_{\mathrm{W},i}\le P^{t_0}_{\mathrm{W},i}+L^{+}_{\mathrm{RP},i}C_{\mathrm{W},i}\right\} \tag{17}$$

$$\begin{cases}P^{\mathrm{up}}_{\mathrm{G},j}=\min\left\{P^{t_0}_{\mathrm{G},j}+dP_{\mathrm{G},j}T_2,P^{\max}_{\mathrm{G},j}\right\}\\ P^{\mathrm{dn}}_{\mathrm{G},j}=\max\left\{P^{t_0}_{\mathrm{G},j}-dP_{\mathrm{G},j}T_2,P^{\min}_{\mathrm{G},j}\right\}\end{cases} \tag{18}$$

In the proposed RPLs model, the outer minimization part of the objective function aims to maximize the operating range of the wind farms, while the inner *max-min* part guarantees the feasibility of the worst case within wind power output set **O** decided by the RPLs solution obtained [12]. (4)-(5) are the bounds of RPLs based on the current power outputs and rated capacities of the wind farms, (6)-(7) are the bounds of active and reactive power outputs of the generators, (8)-(16) are the power flow constraints in conic quadratic format [13], (17) describes the uncertainty set of wind power generation defined by the RPLs, and (18) calculates the active power bounds of generators based on their reserve capacities and ramp rates before the optimization.

The RPLs model presented above aims to determine the uncertainty set, instead of considering optimal solution under a predetermined uncertainty set. So, substitution with a new variable v_i is presented as [11]:

$$P^{t}_{\mathrm{W},i}=P^{t_0}_{\mathrm{W},i}+v_iL^{+}_{\mathrm{RP},i}C_{\mathrm{W},i}+(1-v_i)L^{-}_{\mathrm{RP},i}C_{\mathrm{W},i},\ \forall v_i\in[0,1] \tag{19}$$

Then, a standard three-stage optimization problem with a predetermined uncertainty set is obtained by substituting (19) into the problem presented in (3)-(18):

$$\min_{L^{+}_{\mathrm{RP},i},L^{-}_{\mathrm{RP},i}}\left[\sum_{i\in\mathbf{W}}\left(L^{-}_{\mathrm{RP},i}-L^{+}_{\mathrm{RP},i}\right)+\max_{v_i\in[0,1]}\ \min_{\substack{P^{t}_{\mathrm{W},i},P^{t}_{\mathrm{G},j},Q^{t}_{\mathrm{G},j},\\ p_{nm},q_{nm},c_{nm},s_{nm}}} 0\right] \tag{20}$$

$$s.t.\quad (4)\text{-}(16),\ (18)\text{-}(19)$$

The problem can be divided into a master problem and a subproblem. The master problem is the minimization problem to obtain a set of RPLs.

$$\textbf{MP1:}\quad \begin{aligned}&\min_{x}\ f(x)=\sum_{i\in\mathbf{W}}\left(L^{-}_{\mathrm{RP},i}-L^{+}_{\mathrm{RP},i}\right)\\ &s.t.\ \ \mathbf{C}x\le c\end{aligned} \tag{21}$$

where x represents the $L^{+}_{\mathrm{RP},i}$ and $L^{-}_{\mathrm{RP},i}$ of all wind farms, $\mathbf{C}$ and c are the matrix and vector representing the constraints (4)-(5).

The subproblem is the *max-min* problem to evaluate the feasibility of the RPL solutions obtained from the master problem, which is a robust SOCP problem.

$$\textbf{SP1:}\quad \begin{aligned}&\max_{v\in\mathbf{V}}\ \min_{y\in\mathbf{Y}(v,\hat{x})} 0\\ &s.t.\ \ \mathbf{D}y\le d\\ &\qquad\ \ \mathbf{E}y=e\\ &\qquad\ \ \mathbf{Q}_{\hat{x}}v+\mathbf{R}_{\hat{x}}+\mathbf{H}y=h\\ &\qquad\ \ y\in\mathbf{K}\end{aligned} \tag{22}$$

where $\hat{x}$ is the solution from MP1, v represents v_i of all wind farms within the set of $\mathbf{V}$, and y represents the collection of $P^{t}_{\mathrm{W},i}$, $P^{t}_{\mathrm{G},j}$, $Q^{t}_{\mathrm{G},j}$ p_{nm}, q_{nm}, c_{nm}, and s_{nm} based on $\hat{x}$ and v. $\mathbf{D}$ and d are the matrix and vector representing constraints (6)-(8), $\mathbf{E}$ and e are the matrices and vector representing constraints (9)-(14), $\mathbf{Q}_{\hat{x}}$, $\mathbf{R}_{\hat{x}}$, and h are the matrices and vector representing constraint (19), and $\mathbf{K}$ is the convex cone representing second-order conic constraints (15)-(16).

B. C&CG-based Solution Method

The proposed RPLs model is a robust SOCP problem with the AC power flow formulation, so it cannot be solved efficiently like a robust linear optimization problem with the Benders' decomposition algorithm. As the RPLs optimization problem only needs to guarantee the feasibility of the worst case and has no optimality concern in the subproblem, a C&CG-based solution method is applied in this paper to efficiently solve the proposed robust SOCP problem [17]. The core idea is to find the worst case when the RPLs solution from

the master problem is infeasible in the subproblem, then add new variables and constraints that represent the worst case to the master problem, until a feasible RPLs solution is obtained.

First, a feasibility check subproblem is formulated to obtain the value of v for the worst case based on SP1.

$$\begin{aligned} &\max_{v\in\mathbf{V}} \min_{y\in\mathbf{Y}(v,\hat{x}),r} \mathbf{1}^T\mathbf{r} \\ &s.t.\quad \mathbf{D}y + r_1 \le d && --\mu \\ &\qquad \mathbf{E}y + r_2^+ - r_2^- = e && --\lambda \\ &\qquad \mathbf{Q}_{\hat{x}}v + \mathbf{R}_{\hat{x}} + \mathbf{H}y + r_3^+ - r_3^- = h && --\eta \\ &\qquad y \in \mathbf{K} && --s \end{aligned} \tag{23}$$

where $\mathbf{r} = \left[r_1; r_2^+; r_2^-; r_3^+; r_3^-\right]$ is the vector of slack variables and $\mathbf{1}$ is the unit vector. μ, λ, η, and s are the dual variables of the constraints.

In subproblem (23), the third-stage minimization problem can be transformed into the dual form [26] and combined with the second-stage maximization problem as

$$\begin{aligned} &\max_{v,\mu,\lambda,\eta} \left[\mu^T d + \lambda^T e + \eta^T (h - \mathbf{R}_{\hat{x}} - \mathbf{Q}_{\hat{x}} v)\right] \\ &s.t.\quad \mathbf{D}^T\mu + \mathbf{E}^T\lambda + \mathbf{H}^T\eta + s = \mathbf{0} \\ &\qquad -\mathbf{1} \le \mu \le \mathbf{0}, -\mathbf{1} \le \lambda \le \mathbf{1}, -\mathbf{1} \le \eta \le \mathbf{1}, \\ &\qquad s \in \mathbf{K}^*, v \in \mathbf{V} \end{aligned} \tag{24}$$

where $\mathbf{K}^* = \left\{s : y^T s \ge 0, \forall y \in \mathbf{K}\right\}$ is the cone dual to $\mathbf{K}$. An example of the dual form of an SOCP problem is provided in the Appendix.

The objective function of the subproblem (24) is bilinear due to the bilinear component $\eta^T\mathbf{Q}_x v$. A robust solution is guaranteed to be feasible for all interior points of the polyhedron representing the uncertainty set if it is feasible for all extreme points of the polyhedron, so $\eta^T\mathbf{Q}_x v$ can be transformed by using a big-M formulation [27]. The subproblem (24) can then be reformulated into a mixed-integer second-order conic programming (MISOCP) problem by adding a new variable γ_i to replace $\eta_i v_i$ and letting v_i be a binary variable:

$$\begin{aligned} &\max_{v,\mu,\lambda,\eta,\gamma} \left[\mu^T d + \lambda^T e + \eta^T (h - \mathbf{R}_{\hat{x}}) - \sum_{i\in\mathbf{W}} \gamma_i Q_{\hat{x},ii}\right] \\ &s.t.\quad \mathbf{D}^T\mu + \mathbf{E}^T\lambda + \mathbf{H}^T\eta + s = \mathbf{0} \\ \textbf{SP2:}\quad &\begin{cases} \gamma_i - \eta_i + (1-v_i)\mathrm{M} \ge 0 \\ \gamma_i - \eta_i - (1-v_i)\mathrm{M} \le 0 \\ \gamma_i + v_i\mathrm{M} \ge 0 \\ \gamma_i - v_i\mathrm{M} \le 0 \end{cases}, \forall i \in \mathbf{W} \\ &-\mathbf{1} \le \mu \le \mathbf{0}, -\mathbf{1} \le \lambda \le \mathbf{1}, -\mathbf{1} \le \eta \le \mathbf{1}, \\ &s \in \mathbf{K}^*, v_i = \{0,1\}, \forall i \in \mathbf{W} \end{aligned} \tag{25}$$

where M is the big-M value.

If the objective of SP2 equals zero, it means the subproblem SP1 is feasible. Otherwise, a set of $\hat{v}^l$ that represents the worst case l within the operating ranges decided by the current RPLs solution can be obtained from SP2. Then, a set of new variables and constraints are added to the master problem based on the C&CG method as

$$\begin{aligned} &\min_{x,y^l} f(x) \\ \textbf{MP2:}\quad &s.t.\quad Cx \le c \\ &\begin{cases} \mathbf{D}y^l \le d,\ l = 1,\ldots,\alpha \\ \mathbf{E}y^l = e,\ l = 1,\ldots,\alpha \\ \mathbf{Q}_x\hat{v}^l + \mathbf{R}_x + \mathbf{H}y^l = h,\ l = 1,\ldots,\alpha \\ y^l \in \mathbf{K}^l,\ l = 1,\ldots,\alpha \end{cases} \end{aligned} \tag{26}$$

The new master problem MP2 becomes an SOCP problem. The complete solution method is summarized in Fig. 3.

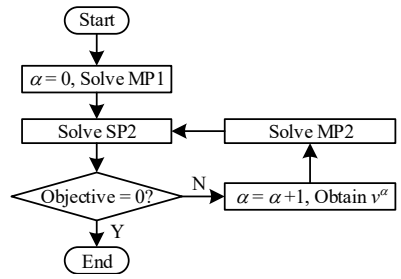

Fig. 3. C&CG-based solution method for RPLs model.

C. Pareto Optimality-based RPLs Evaluation

With the RPLs model and solution method presented above, the maximum total operating range represented by the RPLs can be obtained. However, it does not consider the RPL for each wind farm individually, which would result in unbalanced RPLs for some wind farms. For example, some wind farms may be assigned a very narrow operating range, or even not allowed to ramp up or ramp down, while others are allowed to operate from zero to their rated capacities.

Pareto optimality is a method to deal with the allocation of limited resources [28]. Pareto improvement is defined as a change to a different allocation that makes at least one individual better off without making any other individual worse off, given a certain initial allocation of goods among a set of individuals. An allocation is defined as Pareto optimal when no further Pareto improvements can be made. By applying Pareto optimality, we can find the possible improvement in RPLs of wind farms without narrowing the RPLs of other wind farms, based on a certain initial allocation. A Pareto optimality-based approach for evaluation of RPLs is presented as follows.

Step 1: Set $k = 0$ and $\mathcal{I} = \mathbf{W}$, where $\mathcal{I}$ represents the set of wind farms that can execute a Pareto improvement.

Step 2: Add constraints$\{L_{\mathrm{RP},i}^+ = L_{\mathrm{RP},j}^+, L_{\mathrm{RP},i}^- = L_{\mathrm{RP},j}^-, i, j \in \mathcal{I}\}$ to the master problem to make the RPLs for wind farms in $\mathcal{I}$ equal. Solve the model to obtain $L_{\mathrm{RP},i}^{k+}$ and $L_{\mathrm{RP},i}^{k-}$ for all wind farms as benchmarks. Delete the added equality constraints and add new constraints $\left\{L_{\mathrm{RP},i}^+ \ge L_{\mathrm{RP},i}^{k+}, L_{\mathrm{RP},i}^- \le L_{\mathrm{RP},i}^{k-}, i \in \mathbf{W}\right\}$ to the master problem.

Step 3: For each $i \in \mathcal{I}$, test if there is a Pareto improvement of $L_{\mathrm{RP},i}^+$ ($L_{\mathrm{RP},i}^+ > L_{\mathrm{RP},i}^{k+}$) or $L_{\mathrm{RP},i}^-$($L_{\mathrm{RP},i}^- < L_{\mathrm{RP},i}^{k-}$). If yes, then keep i in set $\mathcal{I}$; if not, delete element i from set $\mathcal{I}$.

Step 4: If there is more than one element in set $\mathcal{I}$, let $k = k + 1$, go back to **Step 2** to find the Pareto improvement, and update the benchmarks. If set $\mathcal{I}$ has only one element or is empty, then resolve the optimization model to obtain the final RPLs.

IV. Evaluation of RRLs

The RPLs of wind farms can ensure the power reserve of generators and the ATCs of transmission lines are sufficient for wind power change under the obtained RPLs. Meanwhile, the adequacy of frequency regulation to handle rapid wind power ramp behavior also needs to be evaluated in terms of RRLs for wind farms. Because the system frequency is a global state variable in a power system and power flow congestion has already been managed in the RPLs model, RRL is considered a unified limit for all wind farms.

Taking a negative wind power ramp event as an example, the typical dynamic frequency response of a single-unit system to a rapid wind power ramp event is shown in Fig. 4.

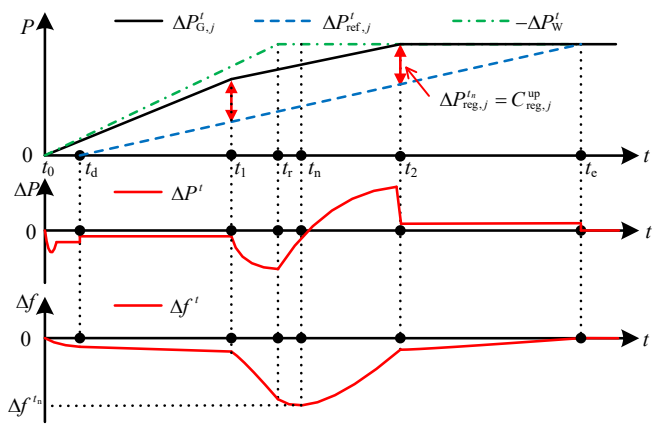

Fig. 4. Dynamic frequency response to a wind power ramp event.

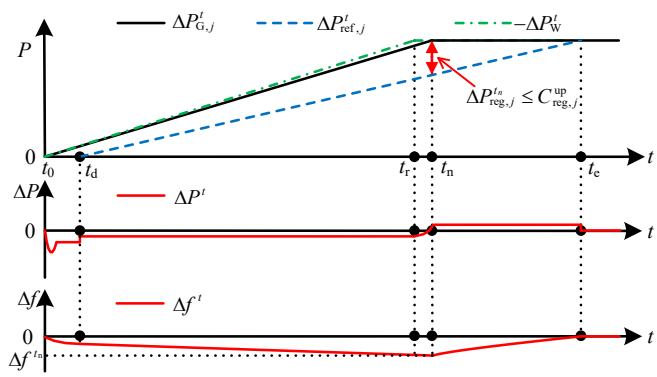

Fig. 5. Dynamic frequency response to a limited wind power ramp event.

The relationship between frequency deviation Δf^t and power imbalance ΔP^t can be described as

$$\frac{d\Delta f^t}{dt} = \frac{1}{M}\Delta P^t = \frac{1}{M}\left(\Delta P^t_{G,j} + \Delta P^t_W - \Delta P^t_D\right) \tag{27}$$

Assume the negative wind power ramp event starts at a time t_0 with a ramp rate of L^-_{RR} ($L^-_{RR} \le 0$) and stops at time t_r, where $t_r - t_0$ is the length of RRL evaluation time T_1. The wind power change is formulated as

$$\Delta P^t_W = \begin{cases} L^-_{RR} C_W \left(t - t_0\right) & t_0 \le t \le t_r \\ L^-_{RR} C_W T_1 & t > t_r \end{cases} \tag{28}$$

Assuming the load demand remains the same during this short period, the change in load can be described with load damping as

$$\Delta P^t_D = D \cdot \Delta f^t \tag{29}$$

The response from the generator consists of two parts, i.e., the change of power reference by AGC and the PFR response:

$$\Delta P^t_{G,j} = \Delta P^t_{ref,j} + \Delta P^t_{reg,j} \tag{30}$$

Considering the maximum ramping capability of the generator, the change of power reference can be described as

$$\Delta P^t_{ref,j} = \begin{cases} 0 & t_0 \le t \le t_d \\ dP_{G,j}\left(t - t_0 - \Delta t_d\right) & t_d < t < t_e \end{cases} \tag{31}$$

where $t_d = t_0 + \Delta t_d$ and t_e is the time that the frequency recovers to the nominal value.

In addition to the ramp rate and upper and lower limits, there are also limited regulation reserve capacities for a generator to participate in PFR [29]. So, the PFR response from a generator can be obtained from

$$\Delta P^t_{reg,j} = \begin{cases} C^{up}_{reg,j} & -\Delta f^t / R_j > C^{up}_{reg,j} \\ -\Delta f^t / R_j & -C^{dn}_{reg,j} \le -\Delta f^t / R_j \le C^{up}_{reg,j} \\ -C^{dn}_{reg,j} & -\Delta f^t / R_j < -C^{dn}_{reg,j} \end{cases} \tag{32}$$

After time t_r, wind power stops ramping up and the power output of the generator continues to increase. As a result, the power imbalance reaches zero at time t_n and the frequency nadir occurs:

$$\Delta P^{t_n}_{ref,j} + \Delta P^{t_n}_{reg,j} + \Delta P^{t_n}_W - \Delta P^{t_n}_D = 0 \tag{33}$$

As shown in Fig. 4, PFR will be able to handle the power imbalance before $\Delta P^t_{reg,j}$ reaches its upper or lower limit. The power imbalance between generation and load will be limited to an acceptable level, which is caused by the response delay of the governor. As a result, the corresponding rate of change of frequency (RoCoF) and frequency deviation will also be limited.

When the power requirement of PFR exceeds the regulation reserve capacities of the generator, the power imbalance would significantly increase because the generator cannot continue to provide additional power as fast as the wind power ramp rate. Consequently, a rapid decline of frequency will occur, shown as the period between t_1 and t_r in Fig. 4. To prevent the frequency deviation from exceeding the allowable range, insufficient PFR capacity should be avoided, as shown in Fig. 5.

The maximum $\Delta P^t_{reg,j}$ that occurs at time t_n should be less than the regulation capacity to avoid rapid frequency decline:

$$\Delta P^{t_n}_{reg,j} = -\Delta P^{t_n}_{ref,j} - \Delta P^{t_n}_W + \Delta P^{t_n}_D \le C^{up}_{reg,j} + \frac{1}{R_j}\Delta f_0 \tag{34}$$

where Δf_0 is the current frequency deviation that represents the used regulation capacity.

Applying (28), (29), and (31) to (34), we can obtain

$$L^-_{RR} C_W T_1 \ge -dP_{G,j}\left(t_n - t_0 - \Delta t_d\right) - \left(C^{up}_{reg,j} + \frac{1}{R_j}\Delta f_0\right) - D\Delta f^{t_n} \tag{35}$$

Because Δf^{t_n} and t_n are relevant to the wind power ramp rate, two conservative approximations are applied to obtain an explicit expression of the RRL criterion: (1) the load damping can be ignored to obtain a conservative estimate due to its positive effect on frequency regulation; and (2) the time difference between t_r and t_n caused by the response delay of the governor is quite small compared to the time interval T_1,

and $t_{\mathrm{n}} > t_{\mathrm{r}}$, so applying $t_{\mathrm{n}} \approx t_{\mathrm{r}}$ also results in a conservative value of RRL.

Then, a conservative RRL criterion can be obtained as

$$L_{\mathrm{RR}}^{-} \geq -\frac{1}{C_{\mathrm{W}} T_1}\left[dP_{\mathrm{G},j}\left(T_1-\Delta t_{\mathrm{d}}\right)+C_{\mathrm{reg},j}^{\mathrm{up}}+\frac{1}{R_j}\Delta f_0\right] \quad (36)$$

Meanwhile, we also need to ensure the frequency nadir does not exceed the frequency limit. When the power imbalance reaches zero at time t_{n}, as presented in (33), we have

$$\Delta f^{t_{\mathrm{n}}} = \frac{dP_{\mathrm{G},j}\left(t_{\mathrm{n}}-t_0-\Delta t_{\mathrm{d}}\right)+L_{\mathrm{RR}}^{-} C_{\mathrm{W}} T_1}{1/R_j+D}+\Delta f_0 \geq \Delta f_{\mathrm{lb}} \quad (37)$$

With $t_{\mathrm{n}} \approx t_{\mathrm{r}}$, we can obtain

$$L_{\mathrm{RR}}^{-} \geq -\frac{dP_{\mathrm{G},j}\left(T_1-\Delta t_{\mathrm{d}}\right)-\left(1/R_j+D\right)\Delta f_{\mathrm{lb}}'}{C_{\mathrm{W}} T_1} \quad (38)$$

where $\Delta f_{\mathrm{lb}}' = \Delta f_{\mathrm{lb}} - \Delta f_0$.

Considering that the power output limit of each generator and the total ramp power in T_1 should be less than the RPLs, the negative RRL of a multi-unit system can be evaluated by considering the PFR capacity criterion L_{RR1}^{-}, the frequency nadir criterion L_{RR2}^{-}, and the RPLs criterion L_{RR3}^{-}.

$$L_{\mathrm{RR}}^{-} = \max\left\{L_{\mathrm{RR1}}^{-}, L_{\mathrm{RR2}}^{-}, L_{\mathrm{RR3}}^{-}\right\} \quad (39)$$

where

$$L_{\mathrm{RR1}}^{-} = -\frac{\sum_{j\in\mathbf{G}} \min\left\{P_{\mathrm{G},j}^{\max}-P_{\mathrm{G},j}^{t_0}, dP_{\mathrm{G},j}\left(T_1-\Delta t_{\mathrm{d}}\right)+C_{\mathrm{reg},j}^{\mathrm{up}}+\frac{\Delta f_0}{R_j}\right\}}{C_{\mathrm{W}} T_1} \quad (40)$$

$$L_{\mathrm{RR2}}^{-} = -\frac{\sum_{j\in\mathbf{G}} \min\left\{P_{\mathrm{G},j}^{\max}-P_{\mathrm{G},j}^{t_0}, dP_{\mathrm{G},j}\left(T_1-\Delta t_{\mathrm{d}}\right)-\frac{\Delta f_{\mathrm{lb}}'}{R_j}\right\}-D\Delta f_{\mathrm{lb}}'}{C_{\mathrm{W}} T_1} \quad (41)$$

$$L_{\mathrm{RR3}}^{-} = -\frac{1}{C_{\mathrm{W}} T_1}\cdot\sum_{i\in\mathbf{W}} L_{\mathrm{RP},i}^{-} C_{\mathrm{W},i} \quad (42)$$

Similarly, we can obtain the positive RRL criterion as

$$L_{\mathrm{RR}}^{+} = \min\left\{L_{\mathrm{RR1}}^{+}, L_{\mathrm{RR2}}^{+}, L_{\mathrm{RR3}}^{+}\right\} \quad (43)$$

where

$$L_{\mathrm{RR1}}^{+} = \frac{\sum_{j\in\mathbf{G}} \min\left\{P_{\mathrm{G},j}^{t_0}-P_{\mathrm{G},j}^{\min}, dP_{\mathrm{G},j}\left(T_1-\Delta t_{\mathrm{d}}\right)+C_{\mathrm{reg},j}^{\mathrm{dn}}-\frac{\Delta f_0}{R_j}\right\}}{C_{\mathrm{W}} T_1} \quad (44)$$

$$L_{\mathrm{RR2}}^{+} = \frac{\sum_{j\in\mathbf{G}} \min\left\{P_{\mathrm{G},j}^{t_0}-P_{\mathrm{G},j}^{\min}, dP_{\mathrm{G},j}\left(T_1-\Delta t_{\mathrm{d}}\right)+\frac{\Delta f_{\mathrm{ub}}'}{R_j}\right\}+D\Delta f_{\mathrm{ub}}'}{C_{\mathrm{W}} T_1} \quad (45)$$

$$L_{\mathrm{RR3}}^{+} = \frac{1}{C_{\mathrm{W}} T_1}\cdot\sum_{i\in\mathbf{W}} L_{\mathrm{RP},i}^{+} C_{\mathrm{W},i} \quad (46)$$

$$\Delta f_{\mathrm{ub}}' = \Delta f_{\mathrm{ub}} - \Delta f_0 \quad (47)$$

V. Case Studies

To verify the effectiveness of the proposed WPRLs evaluation, a modified IEEE 9-bus system integrated with three wind farms and a modified UIUC 150-bus system integrated with ten wind farms are presented for simulation and analysis. The proposed SOCP problem and MISOCP problem are solved by the CPLEX solver.

A. 9-bus System

As shown in Fig. 6, three wind farms are added at buses 3, 6, and 7 to represent wind farms integrated in different kinds of buses, i.e., generation bus, load bus, and transmission bus. The capacity limits of transmission lines are also indicated in Fig. 6. The technical data for power generations are presented in Table I. The reactive power output bounds of conventional generators are set as [–300 MVAR, 300 MVAR] and the power factors of wind farms are set as 1. The allowed voltage bounds of all buses are [0.9 p.u., 1.1 p.u.]. The wind power penetration is about 30% of total installed capacity to represent a power system with high wind power penetration. The current system operating conditions of the wind farms, generators, and loads are presented in Table II.

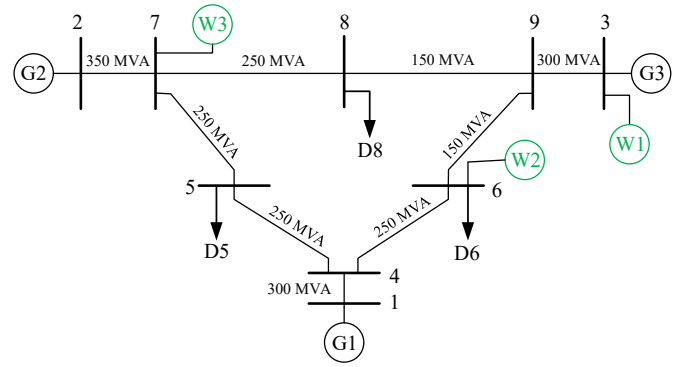

Fig. 6. Modified IEEE 9-bus system with wind farm integration.

TABLE I
TECHNICAL DATA FOR POWER GENERATIONS

No.	$C_{\mathrm{W},i}$ (MW)	$P_{\mathrm{G},j}^{\max}$ (MW)	$P_{\mathrm{G},j}^{\min}$ (MW)	$C_{\mathrm{reg},j}^{\mathrm{up}}$ (MW)	$C_{\mathrm{reg},j}^{\mathrm{dn}}$ (MW)	$dP_{\mathrm{G},j}$ (MW/min)
1	150	250	50	10	10	5
2	100	300	100	15	15	6
3	100	270	100	12	12	6
Total	350	820	250	37	37	17

TABLE II
CURRENT SYSTEM OPERATING CONDITIONS

No.	$P_{\mathrm{W},i}^{t_0}$ (MW)	$P_{\mathrm{G},j}^{t_0}$ (MW)	$P_{\mathrm{D},k}^{t_0}$ (MW)	$P_{\mathrm{Loss}}^{t_0}$ (MW)
1	125	205	350	-
2	80	275	250	-
3	75	165	300	-
Total	280	645	900	25

1) Evaluation of RPLs

The evaluation of RPLs of the wind farms using the proposed method is presented in Table III. An approach [11] that only considers maximizing the total operating power range is used as the benchmark. The two approaches lead to different operating ranges for individual wind farms, as shown in Table III.

The upper power bounds of all wind farms are 100% for the two approaches due to the high percentages of current wind power generation and the sufficient downward spinning reserve capacity. However, the total capacity of the conventional generators is less than the load demand. So it is not acceptable that all wind farms decrease their power output to zero.

The total downward operating range is 178.65 MW with the benchmark approach and 172.65 MW with the proposed approach. The benchmark approach realizes a larger total

operating range; however, the operating ranges for different wind farms are quite unbalanced. WF1 is allowed to operate from 0 to 100% and WF3 also has a –53.65% of downward operating range. WF2 is not allowed to reduce its power output at all (80~100%), which is too strict and obviously not the actual allowed operating range for WF2. Therefore, this approach cannot reflect the operational adequacy of the power system.

TABLE III
RPLS EVALUATION OF WIND FARMS FOR IEEE 9-BUS SYSTEM

Approach	*WF No.*	*Current Power Output* (%)	$L^{-}_{\mathrm{RP},i}$ (%)	$L^{+}_{\mathrm{RP},i}$ (%)	*Operating Range* (%)
Benchmark	WF1	83.33	– 83.33	16.67	0~100
	WF2	80	0	20.00	80~100
	WF3	75	– 53.65	25.00	21.35~100
Proposed Approach	WF1	83.33	– 64.46	16.67	18.87~100
	WF2	80	– 37.98	20.00	42.02~100
	WF3	75	– 37.98	25.00	37.02~100

As shown in Table III, the RPLs solution assigned by the proposed approach based on the Pareto optimality provides a flexible and bidirectional operating range for each wind farm, that considers the operating restrictions of each wind farm as well as the whole power system.

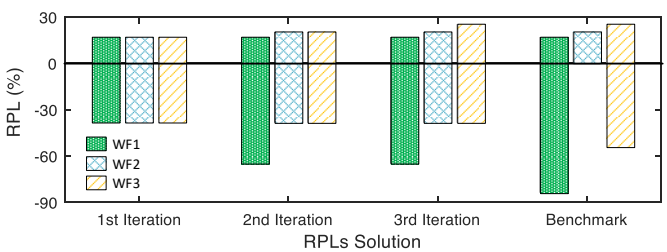

Fig. 7. Iteration process of the Pareto optimality-based RPLs evaluation for the IEEE 9-bus system.

The iteration process of the proposed Pareto optimality-based RPLs evaluation is shown in Fig. 7. The RPLs obtained from the benchmark approach are also presented for comparison. It takes three iterations to obtain the final positive RPLs, due to the differences in power output percentages of the three wind farms. For the negative RPLs, a uniform negative RPL of –37.98% is obtained for all wind farms after the first iteration. The total corresponding reduced wind power is 132.93 MW and leads to a net load of 752.93 MW, which is still less than the total capacity of conventional generators. In the second iteration, a Pareto improvement is only applied for WF1 to achieve an $L^{-}_{\mathrm{RP},1}$ of –64.46%, while maintaining $L^{-}_{\mathrm{RP},2}$ and $L^{-}_{\mathrm{RP},3}$ at –37.98%. The total corresponding reduced wind power becomes 172.65 MW, and the operating range of WF1 is extended without narrowing the RPLs of the other wind farms.

To verify the validity and fairness of the evaluated RPLs, Tables IV and V presents the operating conditions of power generations and transmission lines with the minimum wind power outputs based on the evaluated RPLs and modified RPLs. The modified RPLs solution tries to realize a more balanced RPLs allocation by transferring a small amount of the operating range of WF1 to WF2 and WF3, while keeping the total operating power range the same. With the evaluated negative RPLs, the generation and load are balanced with a power loss of 27.35 MW. Branch 3-9 and Branch 9-8 are fully loaded, but none of the transmission lines are overloaded. With the modified negative RPLs, the total wind generation and the active power output of the generators remain the same but the power flow distribution is changed. An overload occurs on branch 3-9.

This means that the modified RPLs would lead to a violation of the ATC constraints and the evaluated RPLs are already the most balanced solution for the wind farms.

TABLE IV
GENERATION CONDITIONS WITH DIFFERENT RPLS

RPLs Solution	*No.*	$L^{-}_{\mathrm{RP},i}$ (%)	$P^{t}_{\mathrm{W},i}$ (MW)	$P^{t}_{\mathrm{G},j}$ (MW)	$Q^{t}_{\mathrm{G},j}$ (MVAR)
Evaluated RPLs	1	– 64.46	28.31	250	132.23
	2	– 37.98	42.02	300	112.97
	3	– 37.98	37.02	270	31.85
	Total	– 49.33	107.35	820	277.05
Modified RPLs	1	– 63.77	29.35	250	131.50
	2	– 38.50	41.50	300	111.90
	3	– 38.50	36.50	270	33.20
	Total	– 49.33	107.35	820	275.60

TABLE V
CONDITIONS OF TRANSMISSION LINES WITH DIFFERENT RPLS

Branch No.	*Remaining ATC* (MVA)	
	With Evaluated RPLs	With Modified RPLs
1-4	17.19	17.52
2-7	29.44	29.81
3-9	0	–1.19
6-9	1.44	0.34
9-8	0	0

2) Evaluation of RRLs

The evaluation of RPLs focuses on providing an estimation of the maximum allowed wind power ramp rate that would not cause frequency deviation exceeding the designated range, denoted as [– 0.5 Hz, 0.5 Hz] in this paper.

A comparison of different RRL solutions is presented in Table VI to verify the necessity and validity of the proposed RRLs evaluation approach, including: (1) *RPL-RRLs*: the ramp rate only limited by RPLs, with L^{-}_{RR3} and L^{+}_{RR3} as presented in (42) and (46); (2) *SIM-RRLs*: RRLs obtained from simulation with the system frequency deviation constraints; and (3) *EVA-RRLs*: RRLs evaluated by the proposed approach with (39) and (43).

It should be noted that L^{+}_{RR3} is 4% based on the obtained positive RPLs, which would not lead to an over-threshold of frequency deviation in this case. So, the positive RRLs obtained by the *RPL-RRLs* and *EVA-RRLs* are the same at 4%. For the negative RRL, the maximum frequency deviation Δf will be –3.41 Hz with L^{-}_{RR3} = –9.87% from the *RPL-RRLs*, which is far beyond the designated frequency deviation range. Therefore, it is vital to properly evaluate RRLs to ensure operational security. The negative RRL obtained from the simulation is –6.05%, while the evaluated negative RRL is a bit conservative at –5.79%, which validates the analysis presented in Section IV.

TABLE VI
EVALUATION OF RRLS FOR THE IEEE 9-BUS SYSTEM

Approach	L^{+}_{RR}	*Max.* Δf	L^{-}_{RR}	*Max.* Δf
RPL-RRLs	4.00%	0.02 Hz	– 9.87%	– 3.41 Hz
SIM-RRLs	-	-	– 6.05%	– 0.50 Hz
EVA-RRLs	4.00%	0.02 Hz	– 5.79%	– 0.22 Hz

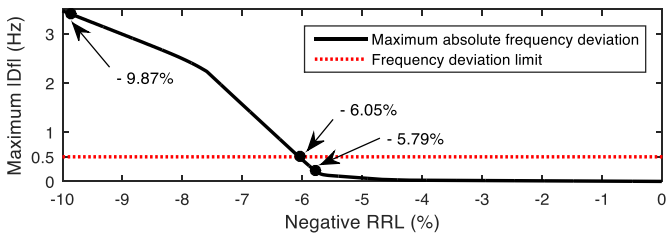

Fig. 8. Maximum absolute frequency deviation with different values of negative RRL for the IEEE 9-bus system.

The maximum absolute frequency deviation with different values of the negative RRL is presented in Fig. 8. A rapid increase of the maximum absolute frequency deviation occurs after the negative RRL exceeds the evaluated value of –5.79%, which is caused by the insufficient of PFR capacity.

Consequently, the RRLs evaluated by the proposed approach are slightly conservative compared to the RRLs obtained by simulation and can avoid the over-threshold of frequency deviation caused by rapid wind power ramp behavior.

B. 150-bus System

The effectiveness of the proposed approach in large systems is tested using a modified 150-bus system based on the UIUC 150-bus system [30]. Ten wind farms are installed at different buses in the modified system, as shown in Table VII. To avoid excessive reserve capacity, the generators at buses 1, 110, 119, 122, 123, 128, 133, and 134 are set offline. Then the total capacity of 19 online conventional generators and 10 wind farms are 11,702 MW and 5,100 MW, respectively, which represents a wind power penetration of 30.35% of installed capacity. The total load demand is 12,680 MW, which is supplied by 2,827 MW of wind power generation and 9,853 MW of conventional power generation.

TABLE VII
WIND FARMS CONFIGURATION IN THE 150-BUS SYSTEM

Bus No.	$C_{W,i}$ at Each Bus (MW)
78, 120, 130	400
86, 144, 146	500
60, 128, 137, 140	600

The operating range of each wind farm evaluated by the benchmark approach and the proposed approach, as well as the current power outputs of the wind farms, are presented in Fig. 9. The total operating range of all wind farms is [–1,728.53 MW, 2,093.18 MW] with the benchmark approach and [–1725.83 MW, 2093.18 MW] with the proposed approach. Though a larger total operating range is evaluated with the benchmark approach, WF2 and WF10 have little ramping down permission while most of other wind farms can regulate their power outputs to zero. While the operating ranges evaluated by the proposed method are more balanced across all wind farms and more accurate for evaluating the operational adequacy of the power system. Notably, the differences in RPLs for different wind farms result from the power flow constraints and different power output percentages of the wind farms.

The RRLs and corresponding maximum frequency deviations with the different approaches for the 150-bus system are presented in Table VIII. The *RPL-RRLs* would lead to over-threshold frequency deviations and the *EVA-RRLs* can limit the frequency deviation to ensure the operational security, which is also a bit conservative compared to the *SIM-RRLs*.

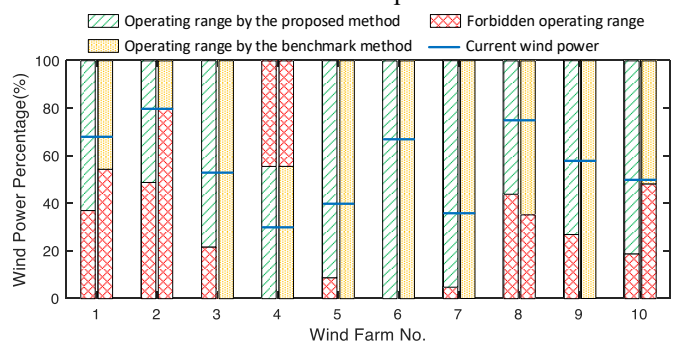

Fig. 9. Operating range of each wind farm for the 150-bus system.

TABLE VIII
EVALUATION OF RRLS FOR THE 150-BUS SYSTEM

Approach	L_{RR}^{+}	*Max.* Δf	L_{RR}^{-}	*Max.* Δf
RPL-RRLs	8.21%	1.32 Hz	– 6.77%	– 1.18 Hz
SIM-RRLs	6.75%	0.50 Hz	– 5.76%	– 0.50 Hz
EVA-RRLs	6.23%	0.13 Hz	– 5.43%	– 0.15 Hz

VI. CONCLUSION

This paper proposed an approach to evaluate WPRLs that can not only provide operating references to wind farms but also evaluate the operational adequacy of a power system by checking the sufficiency of power reserves, ATCs of transmission lines, and frequency regulation capability. As opposed to the existing DNE limit evaluation method, the proposed WPRL evaluation considers AC power flow, the coupled relationship among different wind farms, and RRLs for the system frequency deviation. The simulation results verify that the proposed Pareto optimality-based RPLs evaluation approach can realize a maximum and balanced operating ranges for the wind farms. The frequency deviation analysis indicates that the wind power ramp rate is a non-negligible criterion during power system operation and the proposed RRLs evaluation approach can provide estimated RRLs to avoid the over-threshold of frequency deviation caused by rapid wind power ramp behavior.

APPENDIX

This appendix provides an example of the dual form of an SOCP problem. Assume $X=[x_1,x_2,x_3,x_4]^{\mathrm{T}}$ and J is the number of linear constraints. The primal form and dual form are presented in Table IX.

TABLE IX
PRIMAL FORM AND DUAL FORM OF AN SOCP PROBLEM

Primal Form	Dual Form
$\min \sum_{i=1}^{4} c_i x_i$	$\max \sum_{j=1}^{J} b_j y_j$
$s.t.\ \sum_{i=1}^{4} a_{ji} x_i \le b_j, j=1,..,J$	$s.t.\ \sum_{j=1}^{J} a_{ji} y_j + z_i = c_i, i=1,..,4$
$x_1^2 + x_2^2 \le x_3 x_4$	$z_1^2 + z_2^2 \le z_3 z_4$
$x_3 \ge 0, x_4 \ge 0$	$z_3 \ge 0, z_4 \ge 0, y_j \le 0$

References

[1] T. Aigner, S. Jaehnert, G. L. Doorman, and T. Gjengedal, "The effect of large-scale wind power on system balancing in northern Europe," *IEEE Trans. Sustain. Energy,* vol. 3, no. 4, pp. 751-759, Oct. 2012.

[2] Q. P. Zheng, J. Wang, and A. L. Liu, "Stochastic optimization for unit commitment — a review," *IEEE Trans. Power Syst.,* vol. 30, no. 4, pp. 1913-1924, Jul. 2015.

[3] N. Amjady, S. Dehghan, A. Attarha, and A. Conejo, "Adaptive robust network-constrained AC unit commitment," *IEEE Trans. Power Syst.,* vol. 32, no. 1, pp. 672-683, May 2017.

[4] J. Wu, B. Zhang, K. Wang, J. Shao, J. Yao, D. Zeng, and T. Ge, "Optimal economic dispatch model based on risk management for wind-integrated power system," *IET Gener. Transm. Distrib.,* vol. 9, no. 15, pp. 2152-2158, Nov. 2015.

[5] R. A. Jabr, S. Karaki, and J. A. Korbane, "Robust multi-period OPF with storage and renewables," *IEEE Trans. Power Syst.,* vol. 30, no. 5, pp. 2790-2799, Sep. 2015.

[6] X. Bai, L. Qu, and W. Qiao, "Robust AC optimal power flow for power networks with wind power generation," *IEEE Trans. Power Syst.,* vol. 31, no. 5, pp. 4163-4164, Nov. 2016.

[7] M. A. Hozouri, A. Abbaspour, M. Fotuhi-Firuzabad, and M. Moeini-Aghtaie, "On the use of pumped storage for wind energy maximization in transmission-constrained power systems," *IEEE Trans. Power Syst.,* vol. 30, no. 2, pp. 1017-1025, Mar. 2015.

[8] M. Altin, O. Goksu, R. Teodorescu, P. Rodriguez, B. B. Jensen, and L. Helle, "Overview of recent grid codes for wind power integration," in *Proc. 12th Int. Conf. Optimization Electr. Electron. Equipment*, Brasov, Romania, 2010, pp. 1152-1160.

[9] Nordel, *Nordic Grid Code,* Sweden, 2007. Available: https://www.entsoe.eu.

[10] EirGrid, *Eirgrid Grid Code Version 6.0,* Ireland, 2015. Available: http://www.eirgridgroup.com.

[11] J. Zhao, T. Zheng, and E. Litvinov, "Variable resource dispatch through do-not-exceed limit," *IEEE Trans. Power Syst.,* vol. 30, no. 2, pp. 820-828, Mar. 2015.

[12] A. S. Korad and K. W. Hedman, "Enhancement of do-not-exceed limits with robust corrective topology control," *IEEE Trans. Power Syst.,* vol. 31, no. 3, pp. 1889-1899, May 2016.

[13] R. A. Jabr, "Optimal power flow using an extended conic quadratic formulation," *IEEE Trans. Power Syst.,* vol. 23, no. 3, pp. 1000-1008, Aug. 2008.

[14] C. Zhao, J. Wang, J. P. Watson, and Y. Guan, "Multi-stage robust unit commitment considering wind and demand response uncertainties," *IEEE Trans. Power Syst.,* vol. 28, no. 3, pp. 2708-2717, Aug. 2013.

[15] S. Dehghan, N. Amjady, and A. J. Conejo, "Reliability-constrained robust power system expansion planning," *IEEE Trans. Power Syst.,* vol. 31, no. 3, pp. 2383-2392, May 2016.

[16] L. Fan, J. Wang, R. Jiang, and Y. Guan, "Min-max regret bidding strategy for thermal generator considering price uncertainty," *IEEE Trans. Power Syst.,* vol. 29, no. 5, pp. 2169-2179, Sep. 2014.

[17] B. Zeng and L. Zhao, "Solving two-stage robust optimization problems using a column-and-constraint generation method," *Oper. Res. Lett.,* vol. 41, no. 5, pp. 457-461, Sep. 2013.

[18] A. H. Kasem, E. F. El-Saadany, H. H. El-Tamaly, and M. A. A. Wahab, "Power ramp rate control and flicker mitigation for directly grid connected wind turbines," *IET Renew. Power Gen.,* vol. 4, no. 3, pp. 261-271, May 2010.

[19] H. Banakar, C. Luo, and B. T. Ooi, "Impacts of wind power minute-to-minute variations on power system operation," *IEEE Trans. Power Syst.,* vol. 23, no. 1, pp. 150-160, Feb. 2008.

[20] Y. Liu, W. Du, L. Xiao, H. Wang, and J. Cao, "A method for sizing energy storage system to increase wind penetration as limited by grid frequency deviations," *IEEE Trans. Power Syst.,* vol. 31, no. 1, pp. 729-737, Jan. 2016.

[21] N. Nguyen and J. Mitra, "An analysis of the effects and dependency of wind power penetration on system frequency regulation," *IEEE Trans. Sustain. Energy,* vol. 7, no. 1, pp. 354-363, Jan. 2016.

[22] H. Chavez, M. R. Hezamsadeh, and F. Carlsson, "A simplified model for predicting primary control inadequacy for nonresponsive wind power," *IEEE Trans. Sustain. Energy,* vol. 7, no. 1, pp. 271-278, Jan. 2016.

[23] D. Lee, J. Kim, and R. Baldick, "Stochastic optimal control of the storage system to limit ramp rates of wind power output," *IEEE Trans. Smart Grid,* vol. 4, no. 4, pp. 2256-2265, Dec. 2013.

[24] Hector Chavez, R. Baldick, and S. Sharma, "Governor rate-constrained OPF for primary frequency control adequacy," *IEEE Trans. Power Syst.,* vol. 29, no. 3, pp. 1473-1480, May 2014.

[25] G. Morales-Espana, A. Ramos, and J. Garcia-Gonzalez, "An MIP formulation for joint market-clearing of energy and reserves based on ramp scheduling," *IEEE Trans. Power Syst.,* vol. 29, no. 1, pp. 476-488, Jan. 2014.

[26] S. Boyd and L. Vandenberghe, *Convex optimization*, Cambridge, NY: Cambridge University Press, 2004.

[27] A. S. Korad and K. W. Hedman, "Robust corrective topology control for system reliability," *IEEE Trans. Power Syst.,* vol. 28, no. 4, pp. 4042-4051, Nov. 2013.

[28] P. M. Pardalos, A. Migdalas, and L. Pitsoulis, *Pareto Optimality, Game Theory and Equilibria*, New York, NY: Springer Science & Business Media, 2008.

[29] J. F. Restrepo and F. D. Galiana, "Unit commitment with primary frequency regulation constraints," *IEEE Trans. Power Syst.,* vol. 20, no. 4, pp. 1836-1842, Nov. 2005.

[30] Illinois Center for a Smarter Electric Grid, *UIUC 150-bus system*, [Online]. Available: http://icseg.iti.illinois.edu/synthetic-power-cases/uiuc-150-bus-system/.

Yuzhong Gong (S'13-M'16) received the B.S. and Ph.D. degrees in electrical engineering from Zhejiang University of Technology and Zhejiang University, Hangzhou, China, in 2010 and 2015, respectively.

He is currently a Postdoctoral Fellow in the Department of Electrical and Computer Engineering, University of Saskatchewan, Saskatoon, SK, Canada. His current research interests include the optimization of power system operation and renewable energy integration.

C. Y. Chung (M'01-SM'07-F'16) received the B.Eng. (with First Class Honors) and Ph.D. degrees in electrical engineering from The Hong Kong Polytechnic University, Hong Kong, China, in 1995 and 1999, respectively.

He has worked for Powertech Labs, Inc., Surrey, BC, Canada; the University of Alberta, Edmonton, AB, Canada; and The Hong Kong Polytechnic University, China. He is currently a Professor, the NSERC/SaskPower (Senior) Industrial Research Chair in Smart Grid Technologies, and the SaskPower Chair in Power Systems Engineering in the Department of Electrical and Computer Engineering at the University of Saskatchewan, Saskatoon, SK, Canada. His research interests include smart grid technologies, renewable energy, power system stability/control, planning and operation, computational intelligence applications, power markets and electric vehicle charging.

Dr. Chung is an Editor of *IEEE Transactions on Power Systems and IEEE Transactions on Sustainable Energy* and an Associate Editor of *IET Generation, Transmission, and Distribution*. He is also an IEEE PES Distinguished Lecturer and a Member-at-Large (Global Outreach) of the IEEE PES Governing Board.

R. S. Mall received his B.Eng. in Electrical Engineering from the University of Saskatchewan in 2004 and P.Eng. designation from the Association of Professional Engineers of Saskatchewan in 2008.

Since graduation, he has and continues to work for the Saskatchewan provincial electrical utility (Saskatchewan Power Corporation). His areas of expertise include grid transmission systems, new generation interconnection studies, load interconnection analysis, transmission reliability assessments, reliability compliance, and business development.